PETROVIETNAM JOURNAL
Volume 10/2022, pp. 28 - 34
ISSN 2615-9902

# ANALYSING THE EFFECT OF BEDDING PLANE ORIENTATION ON THE WELLBORE FAILURE

**Nguyen Van Hung[1], Luong Hai Linh[2]**
[1]Phenikaa University
[2]Petrovietnam University
Email: hung.nguyenvan1@phenikaa-uni.edu.vn
https://doi.org/10.47800/PVJ.2022.10-04

## Summary

The paper presents a theory of the "plane of weakness" modelling applied to a deviated borehole that penetrated through laminated shale containing numerous parallel weakness planes. The obtained results show that the strength envelope for anisotropic rock is characterised by a U-shaped reduction in strength for failure along the weakness plane, confining pressure from 20 MPa to 80 MPa whithout any change in the failure mechanism of the shale. In terms of borehole failure, there is a risk zone within the well, whose inclination varies between 60$^o$ - 90$^o$, and the azimuth changes from 100$^o$ - 165$^o$.

**Key words:** Wellbore stability, weakness plane, triaxial compression tests, geomechanics.

## 1. Introduction

Wellbore instability is a common problem in oil and gas exploration/production wells during drilling and leads to large expenses. Rock, a natural solid material, is characterised by its anisotropy due to various factors such as the age of formation, lithology, tectonic, deformation, texture and structure, etc. Particularly, weak bedding planes in a rock mass may affect mechanical properties of the rocks and wellbore stability because of its anisotropic strength [1].

Strength is considered as a major parameter to characterise the rock mechanical behaviour. Most of the studies indicate that the strength anisotropy is influenced by dual interaction of orientation of sample bedding plane with respect to the principal stress and the magnitude of confining pressure [2]. Hence, significant efforts have been paid to further understand the anisotropy behaviour in terms of engineering design and analysis to overcome the difficulties in construction of those projects in the anisotropic rock environments. During the last few years, the isotropic model used to determine the anisotropic rock properties revealed a significant uncertainty and unreliability [3 - 5]. In addition, research on wellbore instability was first conducted upon an assumption of linear elastic, isotropic rock, which does not reflect real condition of a rock mass [6].

Several experiments related to the effect of weak bedding planes on rock strength, pore pressure, wellbore instability analysis, etc. have been conducted, suggesting that the bedding plane orientations affected both the elastic constants and yield strength of the rock [4 - 9]. Okland and Cook [10] developed an anisotropic strength theory for wellbore instability problem in the North Sea oil/gas fields, showing that the wellbore instability became worse when drilling parallelly or sub-parallelly to the bedding planes. The plane of weakness theory has been used by Jin et.al. [11] to determine the stability of horizontal wellbores in a naturally fractured formation during well testing. The results showed that the strike of natural fractures could apparently affect the damage form of the sidewall rocks, and a sidewall adjacent to the area of minimum horizontal stress field orientation was the most ready to collapse. In the shale formation, Wu and Tan [12] illustrated that the strength along bedding planes was much weaker than the intact shale material. Effect of the bedding plane failure on wellbore stability in shale was assessed using a transversely isotropic poroelastic and single plane of weakness model. The obtained results showed that the shale bedding planes mainly affected high angle and horizontal wells, which were drilled close

*Date of receipt: 8/9/2022. Date of review and editing: 8/9 - 4/10/2022.*
*Date of approval: 5/10/2022.*

to the minimum horizontal stress direction. Other researchers [13 - 15] found that the analytical process of well drilling and completion in gas shale bearing weak bedding planes depended on logging data, real-time drilling data and in-situ stress tests.

Other elements can also affect wellbore instability when the well encounters weak bedding planes, e.g., the angle between the wellbore and the weak bedding plane. If the angle is high (~ 70° - 90°), the oblique loading on relatively weak laminations likely leads to premature shear failure. Depending on the relative magnitude of the anisotropic rock strength and borehole stress concentration, the breakouts may occur at positions around the borehole. This response is different from those conventionally found in isotropic rock. Due to overburdened diagenesis, shale commonly demonstrates high pore pressure, alignment of phyllosilicates. For this reason, instability of shale is a serious issue, which potentially causes costly problems in many foothills drilling operations, e.g., slip surfaces failing [7, 13]. Thus, a sufficient understanding of the mechanism for instabilities and lost circulation during drilling is needed to reduce the operation cost.

The results of uniaxial compressive, indirect tensile strength and triaxial tests were conducted based on a variety of failure criteria proposed for anisotropic materials. These theories were classified into three groups: mathematical continuous criteria, empirical continuous models, and discontinuous weakness plane theories. The empirical Hoek-Brown failure criterion was fitted to the triaxial data, the corresponding Mohr-Coulomb failure envelope using friction and cohesion parameters. The single plane of weakness theory proposed by Jaeger et.al. [1] is the most widely known. In this theory, the classic Mohr-Coulomb criterion is used to describe the failure of both the bedding planes.

In this paper, we will outline an anisotropic strength model, the effect of weak bedding plane parameters and in-situ stresses on wellbore failure analysis.

## 2. Modelling

The borehole failure analysis is conducted upon the following assumptions: (i) The rock is heterogeneous and anisotropic; (ii) a set of parallel weak bedding planes exists in which the strengths are low, but the strength of the rock in other directions is uniform; (iii) deformation of rock is low and linear.

### *2.1. Borehole stress*

Before a well is drilled the rock is in a state of equilibrium and the stresses in the Earth under these conditions are known as the far field stresses. Once it is excavated, the static stress state becomes disturbed as the support originally offered by the drilled-out rock is replaced by the hydraulic pressure of the drilling mud and hence causing instability in the rock formation. The disturbed in-situ stress state therefore imposes a different set of stresses in excavation area. Figures 1 and 2 illustrate a schematic distribution of in-situ stresses existing in the formation around a wellbore. The stresses can be resolved into a vertical or overburden stress $\sigma_v$, the maximum horizontal in-situ stress $\sigma_H$, and the minimum horizontal in-situ stress $\sigma_h$, which are generally unequal. The direction of well is modelled as shown in Figure 3.

All of the stress components at the wellbore can be calculated in the following steps: (1) Identify the principal in-situ stress state ($\sigma_v$, $\sigma_H$, $\sigma_h$); (2) Transform the stress state ($\sigma_v$, $\sigma_H$, $\sigma_h$) to the stress state ($\sigma_x$, $\sigma_y$, $\sigma_z$) defined with respect to the Cartesian coordinate system attached to the wellbore (Equations 1a - 1f); (3) Find the local stress state ($\sigma_r$, $\sigma_\theta$, $\sigma_a$) with respect to the cylindrical coordinated system attached to the wellbore at the distance of a from the center of well, in terms of the stress state ($\sigma_x$, $\sigma_y$, $\sigma_z$) (Equations 2a - 2f); (4) Find the stress state at the wellbore ($\sigma_r$, $\sigma_\theta$, $\sigma_a$) (a = r) as Figure 2. For a vertical well, the local stresses can be calculated from the Equations 3a - 3e, as Equations 4a - 4d below:

$$\sigma_x = (\sigma_H cos^2 a_w + \sigma_h sin^2 a_w) cos^2 i_w + \sigma_v sin^2 i_w \quad (1a)$$

$$\sigma_y = \sigma_H sin^2 a_w + \sigma_h cos^2 a_w \quad (1b)$$

$$\sigma_z = (\sigma_H cos^2 a_w + \sigma_h sin^2 a_w) sin^2 i_w + \sigma_v cos^2 i_w \quad (1c)$$

$$\tau_{xy} = \frac{1}{2}(\sigma_H - \sigma_h) sin2a_w cosi_w \quad (1d)$$

$$\tau_{xz} = \frac{1}{2}(\sigma_H cos^2 a_w + \sigma_h sin^2 a_w - \sigma_v) sin2i_w \quad (1e)$$

$$\tau_{yz} = \frac{1}{2}(\sigma_H - \sigma_h) sin2a_w sini_w \quad (1f)$$

$$\sigma_r = \frac{1}{2}(\sigma_x + \sigma_y)\left(1 - \frac{a^2}{r^2}\right) + \frac{1}{2}(\sigma_x - \sigma_y) \quad (2a)$$
$$\left(1 + 3\frac{a^4}{r^4} - 4\frac{a^2}{r^2}\right) cos2\theta + \tau_{xy}\left(1 + 3\frac{a^4}{r^4} - 4\frac{a^2}{r^2}\right) sin2\theta + \frac{a^2}{r^2} P_w$$

$$\sigma_t = \frac{1}{2}(\sigma_x + \sigma_y)\left(1 + \frac{a^2}{r^2}\right) - \frac{1}{2}(\sigma_x - \sigma_y) \quad (2b)$$
$$\left(1 + 3\frac{a^2}{r^2}\right) cos2\theta - \tau_{xy}\left(1 + 3\frac{a^2}{r^2}\right) sin2\theta - \frac{a^2}{r^2} P_w$$

$$\sigma_a = \sigma_z - 2\,\nu(\sigma_x - \sigma_y)\frac{a^2}{r^2}cos2\theta - 4\,\nu\tau_{xy}\frac{a^2}{r^2}sin2\theta \quad (2c)$$

$$\tau_{\theta z} = (\tau_{yz}cos\theta - \tau_{xz}sin\theta)(1 + \frac{a^2}{r^2}) \quad (2d)$$

$$\tau_{r\theta} = [\frac{1}{2}(\sigma_x - \sigma_y)sin2\theta + \tau_{xy}cos2\theta](1 - 3\frac{a^4}{r^4} + 2\frac{a^2}{r^2}) \quad (2e)$$

$$\tau_{rz} = (\tau_{xy}cos\theta + \tau_{yz}sin\theta)(1 - \frac{a^2}{r^2}) \quad (2f)$$

$$\sigma_r = P_w \quad (3a)$$

$$\sigma_t = (\sigma_x + \sigma_y) - 2\,(\sigma_x - \sigma_y)cos2\theta - 4\,\tau_{xy}sin2\theta - P_w \quad (3b)$$

$$\sigma_a = \sigma_z - 2\,\nu(\sigma_x - \sigma_y)cos2\theta - 4\,\nu\tau_{xy}sin2\theta \quad (3c)$$

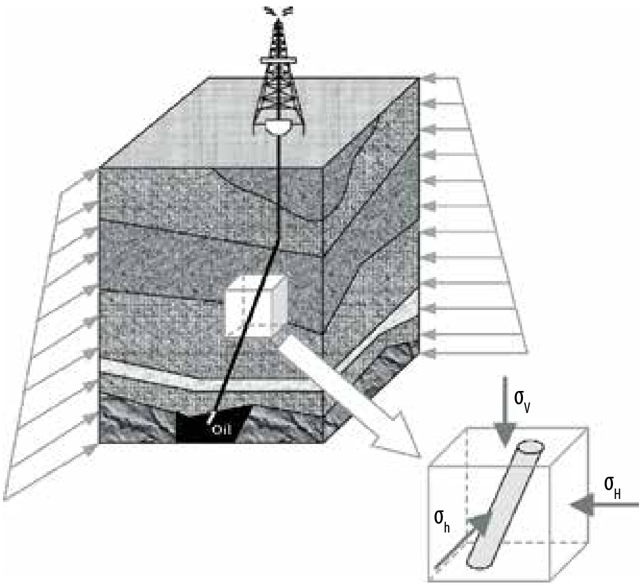


*Figure 1. A scheme showing in-situ stresses around a wellbore [13].*

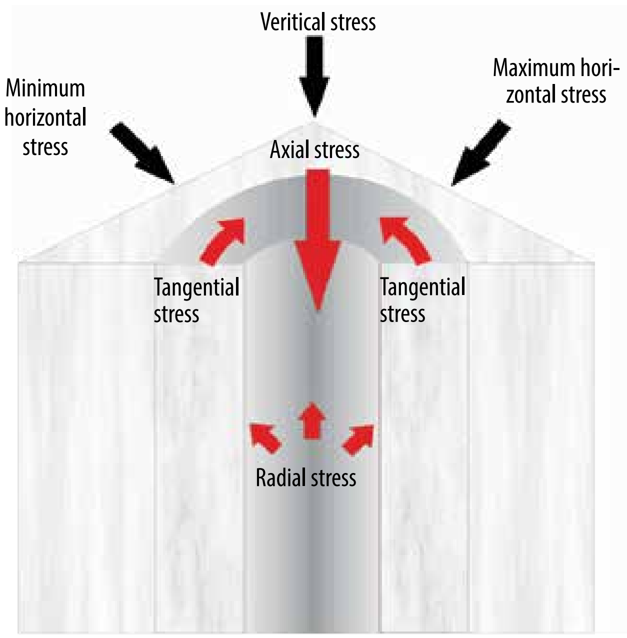


*Figure 2. Position of stresses around a wellbore in the rock formation [14].*

$$\tau_{\theta z} = 2\,(\tau_{yz}cos\theta - \tau_{xz}sin\theta) \quad (3d)$$

$$\tau_{r\theta} = 0;\ \tau_{rz} = 0 \quad (3e)$$

$$\sigma_r = P_w \quad (4a)$$

$$\sigma_t = (\sigma_x + \sigma_y) - 2(\sigma_x - \sigma_y)cos2\theta - P_w \quad (4b)$$

$$\sigma_a = \sigma_z - 2\nu(\sigma_x - \sigma_y)cos2\theta \quad (4c)$$

$$\tau_{\theta z} = 0;\ \tau_{r\theta} = 0;\ \tau_{rz} = 0 \quad (4d)$$

where:

$\sigma_v$: Vertical (overburden) in-situ stress (Pa, psi);

$\sigma_H$: Maximum horizontal in-situ stress (Pa, psi);

$\sigma_h$: Minimum horizontal in-situ stress (Pa, psi);

$\sigma_x$, $\sigma_y$, $\sigma_z$: stress state in the Cartesian coordinate system (Pa, psi);

τ: Shear stress (Pa, psi);

$\sigma_t$: Tensile stress (Pa, psi);

$\sigma_r$: Radius stress (Pa, psi);

$P_w$: Wellbore internal pressure (Pa, psi);

a: Borehole radius (m, in);

r, z, θ: Cylindrical co-ordinate system (m, in);

### *2.2. Anisotropic rock strength*

According to the rock failure applied to planar anisotropy, which is known as "the single plane of

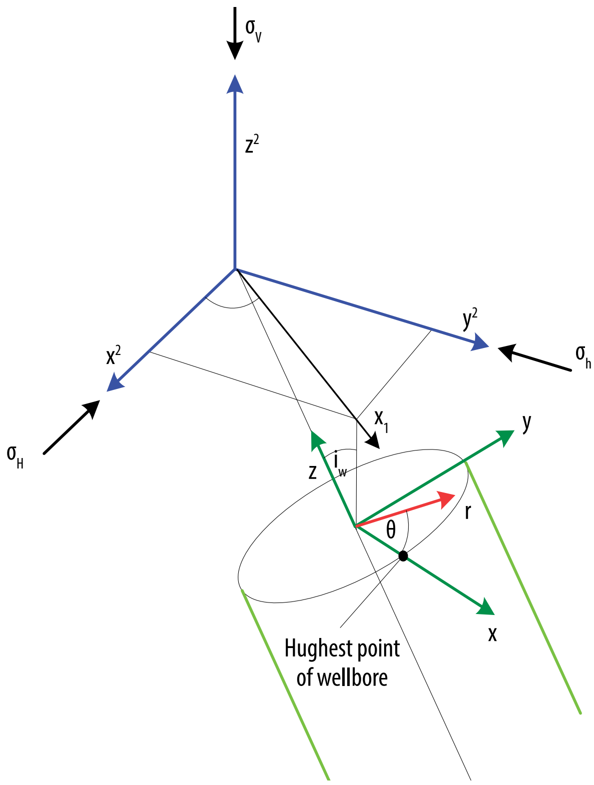


*Figure 3. The coordinate system for the in-situ stress display [14].*

weakness theory", the condition for sliding along these planes is given in Equation 5 [1]:

$$\sigma_1 = \sigma_3 + \frac{2(S_w + \mu_w \sigma_3)}{(1 - \mu_w cos\beta)sin2\beta} \quad (5)$$

where:

$\sigma_1$: Maximum principal stress (Pa, psi);

$\sigma_3$: Minimum principal stress (Pa, psi);

$S_w$: Inherent shear strength of the planes of weakness (Pa, psi);

$\mu_w = tan\varphi_w$: Coefficient of internal friction along weak planes;

$\varphi_w$: Friction angle of weak plane (degrees);

β: Angle between $\sigma_1$ and the normal to the planes of weakness.

Failure will occur in the bulk material based on the same failure criterion as the weak plane such that the maximum principal stress that can be sustained is:

$$\sigma_1 = 2\tau_0^b \frac{cos\varphi^b}{1 - sin\varphi^b} + \sigma_3 \frac{1 + sin\varphi^b}{1 - sin\varphi^b} \quad (6)$$

where:

$\tau_0^b$: Cohesion;

$\varphi^b$: Friction angle of bulk material (degrees).

It is assumed that the bulk material has isotropic strength properties.

## 3. Case study

The data used in this study are derived from pre-existing works conducted by Crawford et.al. [17], with

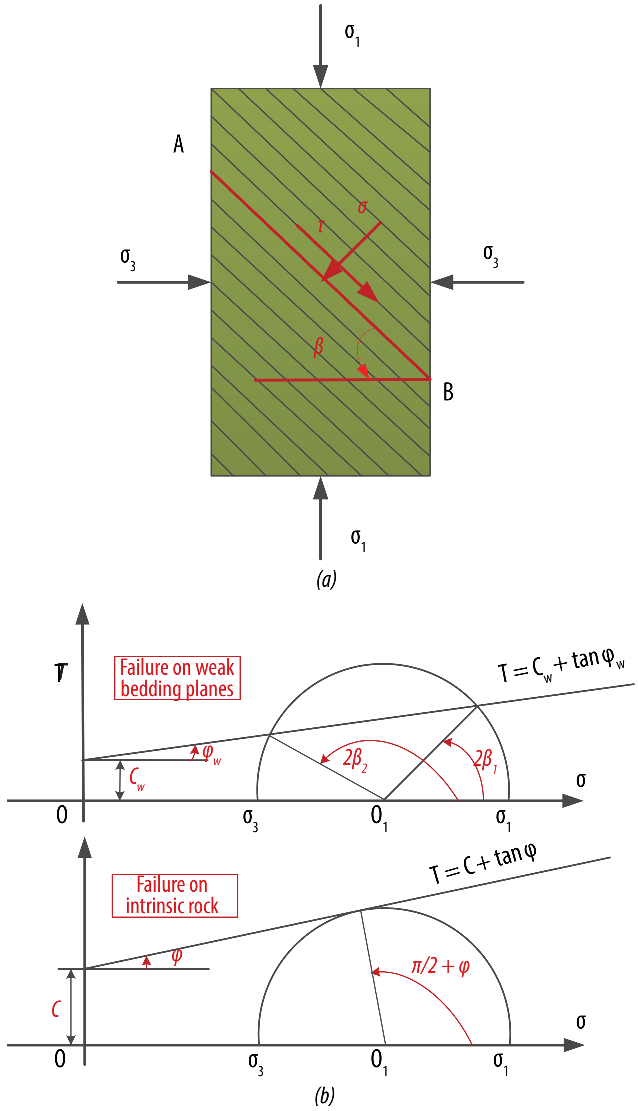


***Figure 4.*** *(a) Stress state of rock containing weak bedding planes; (b) rock strength analysis of failure on weak bedding planes and intrinsic rock [16].*

***Table 1.*** *Summary of 14 database lithologies used in anisotropic shear strength analyses [17]*

| I.D | | Lithology | Source | | ≠triaxial test (β) | Cohesive strength (MPa) | Friction angle (degrees) |
|---|---|---|---|---|---|---|---|
| Lst. | ≠1 | Laminated dolomitic limestone | Outcrop | McGill & Raney | 40 | 93.9 | 29.9 |
| Calcareous shales | ≠2 | Green River oil shale (lean) | Mine | McLamore & Gray | 24 | 59.6 | 31.4 |
| | ≠3 | Green River oil shale (rich) | Mine | McLamore & Gray | 21 | 39.0 | 21.4 |
| | ≠4 | Intra-reservoir marl | Cored well | In-house study | 27 | 30.7 | 20.2 |
| | ≠5 | Intra-reservoir marl | Cored well | In-house study | 28 | 24.4 | 8.1 |
| | ≠6 | Intra-reservoir marl | Cored well | In-house study | 31 | 20.7 | 8.5 |
| Sst. | ≠7 | Fine-grained highly cemented sandstone | Outcrop | Chenevert & Gatlin | 17 | 38.4 | 56.4 |
| Argillaceous shales | ≠8 | Outcrop shale | Outcrop | In-house study | 35 | 29.1 | 29.7 |
| | ≠9 | Top seal shale | Cored well | In-house study | 31 | 18.7 | 9.1 |
| | ≠10 | Top seal shale | Cored well | In-house study | 30 | 17.6 | 5.7 |
| | ≠11 | Top seal shale | Cored well | In-house study " | 28 | 16.4 | 14.8 |
| | ≠12 | Tournemire shale | Outcrop | Niandou et. al. | 25 | 16.8 | 21.7 |
| | ≠13 | Laminated silty mudstone | Mine | Attewell & Farmer | 42 | 14.9 | 33.8 |
| Coal | ≠14 | Barnsley Hards bituminous coal | Mine | Pomeroy et. al. | 28 | 12.6 | 36.3 |

~400 triaxial compression testing on 7 individual lithologies (3 top seal shales, 3 intra-reservoir shales and 1 outcrop shale) [17], Narayanasamy et.al. [18], Chris et.al. [19]. Those studies used samples collected from Terra Novad, Yasar 2001 of the Upper Miocene - Pliocene Handere formation.

### 4. Determination of strength anisotropy

Based on the above models and laboratory data, the strength of rock is analysed first. Figure 5 presents a summary of the tests for shale in Table 1. The failure theory is used for interpretation of the test results for the anisotropic rocks, namely the single plane of weakness theory [1]. The failure stress can be computed by specifying cohesion and friction angle (for varying orientation of β). It is necessary to evaluate two cohesive strength parameters and two coefficients of internal friction for anisotropic materials. As shown in Figure 5, the strength envelope for anisotropic rock is a U-shaped reduction for failure along the weakness plane. At most confining pressures, the criterion overestimates the strength in the regions, where failure is predicted through the intact rock. It is clearly indicated that within the confining pressure varying from 20 MPa to 80 MPa, there is no change in the failure mechanism of the shale. In addition, the results evidently show the anisotropic strength slumped at supreme confining pressure besides, the theoretical method provides advantageous prevision of anisotropy behaviour at higher confining pressures.

### 5. Cohesive strength model

Cohesive strength or cohesion is the strength of bonding between the particles or surfaces that make up the material. In rock mechanics, the cohesive strength is more specifically the inherent shear strength of a plane across which there is no normal stress. In general, this strength parameter is determined in case of no distinction between failure of a weak plane and failure through the bulk material. In this case, the linearised Mohr failure line can be used, and cohesive strength is estimated by uniaxial tests or triaxial tests. According to experimental

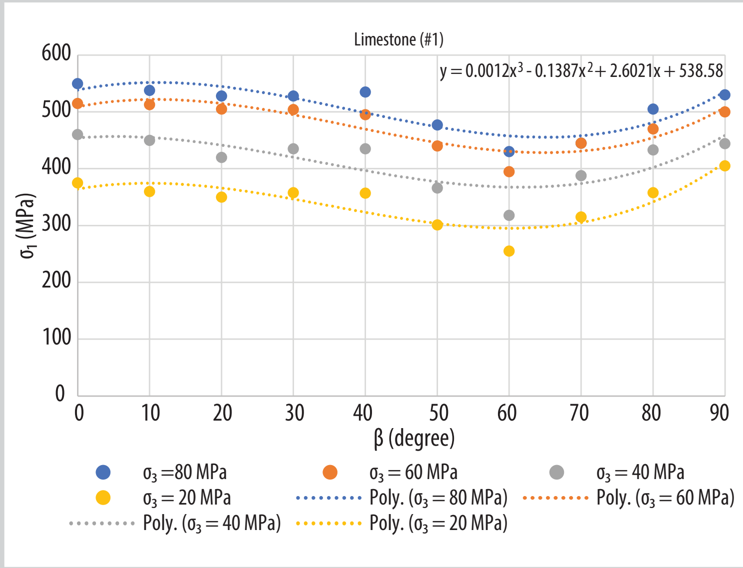


***Figure 5.*** *Single plane of weakness model fits with testing data (solid lines - model, points - laboratory data).*

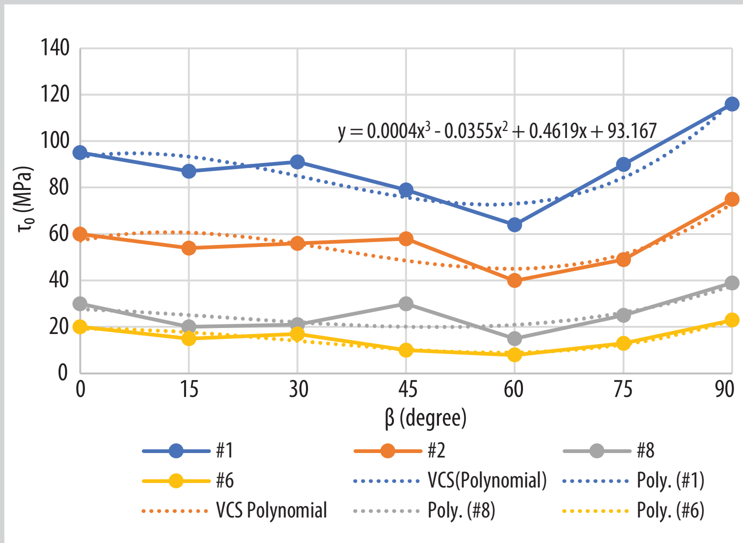


***Figure 6.*** *The cohesive strength model.*

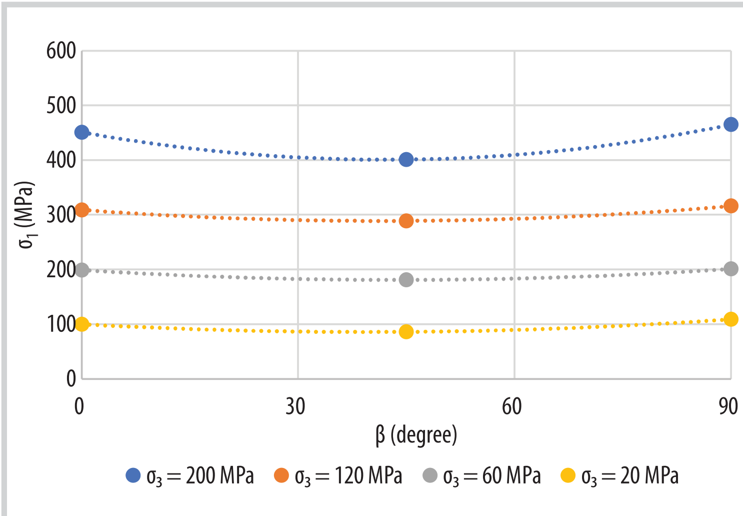


***Figure 7.*** *Maximum principal stress prediction.*

*Table 2. Input data*

| Property | Value |
|---|---|
| Depth (m) | 6,000 |
| Overburden stress (MPa/100 m) | 2.4 |
| Major horizontal stress (MPa/100 m) | 2.08 |
| Minor horizontal stress (MPa/100 m) | 1.9 |
| Pore pressure (MPa) | 70 |
| Cohesion of the weak planes (MPa) | 3.5 |
| Internal friction angle of weak planes (°) | 14 |
| Cohesion strength of rock (MPa) | 18 |
| Internal friction angle (°) | 32 |
| Poisson's ratio | 0.22 |
| Biot's coefficient | 0.9 |
| Wellbore diameter (mm) | 140 |
| Direction of the maximum horizontal principle in-situ stress (°) | 115 |
| Fluid density (g/cm$^3$) | 1.22 |

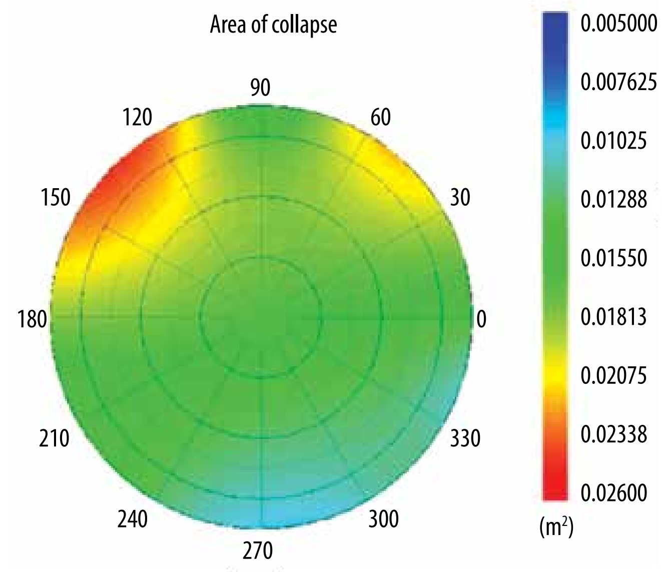


***Figure 8.** Sanding onset in a well of shale formation.*

results (Table 1), the cohesive strength data is considered a function of the third-order polynomial of weak plane angle.

The cohesive strength of shale is determined as shown in Figure 6. The continuous variable cohesive strength criterion produces failure envelopes that predict a continuous change. The cohesion theory can be estimated correctly even with β = 0°, 90°, except at 45° and 75°. By using the polynomial technique, we constate that this technique can be used for predicting the maximum principal stress in function of β angle (Figure 7). This result is much better than the single plane of weakness model.

## 6. Borehole failure

Based on the above models (Equation 5), borehole failure is analysed by applying the data presented in Table 2. The sand production phenomenon is generally taking place through three stages: loss of mechanical integrity of rocks surrounding the borehole, separation of solid particles due to the hydrodynamic force, and transportation of the particles to the surface by production. Excessive sanding or solid production may damage the downhole and surface equipment. Drilling mud is normally chosen in such a way to resist the formation pore pressure, hence preventing the formation fluid from flowing into the wellbore. The drilling mud is not always able to resist the compressive stresses of the wellbore. In this case, shear failures of rock will occur due to the imbalance between stress and rock strength.

In this study, we investigate the possibility of sanding with the presence of weak plane. The returning results allowed us to constate that the field stress regime is normal ($\sigma_v > \sigma_H > \sigma_h$). Figure 8 reveals the possibility of sanding for this case study. As we can see from this figure, the most dangerous case is coded by the red color. In this case, there is a risk zone in the well with the trend angle of weak plane ranging between 60° - 90°, and the changes from 100° - 165°.

However, with any different range of weak plane, the well can be drilled in any azimuth without sanding problem. This result is vital which enables to recommend well plannings, and it is also a good solution for simulation to tackle the risk of drilling well.

## 7. Conclusions

Results are obtained from various tests applied to the anisotropic strength of shale associated with weak planes, and wellbore failure. This study allows us to draw the following conclusions:

The strength envelope for anisotropic rock shows a U-shaped reduction in strength for failure along the weakness plane.

No change in the failure mechanism of the shale is recorded within the 20 - 80 Mpa interval confining pressure.

The cohesion theory can be estimated correctly even with β = 0°, 90°, except at 45° and 75°. By using the polynomial technique, it is possible to provide a correctly prediction of the maximum principal stress in function of β angle.

There is a risk zone in the well with the trend angle of weak plane ranging between 60° - 90°, and the azimuth changing from 100° - 165°.

**References**

[1] John Conrad Jaeger, Neville G.W. Cook, and Robert Zimmerman, *Fundamentals of rock mechanics, 4th edition*. Blackwell Publishers, 2007.

[2] Yong Ming Tien, Ming Chuan Kuo, and Charng Hsein Juang, "An experimental investigation of the failure mechanism of simulated transversely isotropic rocks", *International Journal of Rock Mechanics and Mining Sciences*, Vol. 43, No. 8, pp. 1163 - 1181, 2006. DOI: 10.1016/j.ijrmms.2006.03.011.

[3] Shuai Heng, Yingtong Guo, Chunhe Yang, Jack J. K. Daemen, and Zhi Li, "Experimental and theoretical study of the anisotropic properties of shale", *International Journal of Rock Mechanics and Mining Sciences*, Vol. 74, pp. 58 - 68, 2015.

[4] Jingyi Cheng, Zhijun Wan, Yidong Zhang, Wenfeng Li, Syd S. Peng, and Peng Zhang, "Experimental study on anisotropic strength and deformation behavior of a coal measure shale under room dried and water saturated conditions", *Shock and Vibration*, 2015. DOI: 10.1155/290293.

[5] G. Duveau and J.F. Shao, "A modified single plane of weakness theory for the failure of highly stratified rocks", *International Journal of Rock Mechanics and Mining Sciences*, Vol. 35, No. 6, pp. 807 - 813, 1998. DOI: 10.1016/S0148-9062(98)00013-8.

[6] W.B. Bradley, "Failure of inclined boreholes", *Journal of Energy Resources Technology*, Vol. 101, No. 4, pp. 232 - 239, 1979. DOI: 10.1115/1.3446925.

[7] Brent S. Aadnoy, "Modeling of the stability of highly inclined boreholes in anisotropic rock formations", *SPE Drilling Engineering*, Vol. 3, No. 3, pp. 259 - 268, 1988. DOI: 10.2118/16526-PA.

[8] M.E. Chenevert and C. Gatlin, "Mechanical anisotropies of laminated sedimentary rocks", *SPE Journal*, Vol. 5, No. 1, pp. 67 - 77, 1965. DOI: 10.2118/890-PA.

[9] Vahid Dokhani, Mengjioa Yu, and Stefan Miska, "The effect of bedding plane orientation on pore pressure in shale formations: Laboratory testing and mathematical modeling", *47th U.S. Rock Mechanics/Geomechanics Symposium, San Francisco, 23 - 26 June 2013*.

[10] D. Okland and J.M. Cook, "Bedding related borehole instability in high angle wells", *SPE/ISRM Rock Mechanics in Petroleum Engineering, Norway, 8 - 10 July 1998*. DOI: 10.2118/47285-MS.

[11] Yuanlin Jin, Z. Qi, Mingqing Chen, F. Zhang, Y. Lu, and Bing Hou, "A mechanism study on the fractured reservoir instability during well testing of horizontal wells", *Shiyou Xuebao/Acta Petrologica Sinica*, Vol. 32, No. 2, pp. 295 - 298, 2011.

[12] Bailin Wu and C.P. Tan, "Effect of shale bedding plane failure on wellbore stability – example from analyzing stuck-pipe wells", *44th U.S. Rock Mechanics Symposium and 5th U.S. - Canada Rock Mechanics Symposium, Salt Lake City, Utah, 27 - 30 June 2010*.

[13] Bernt Aadnøy and Reza Looyeh, *Petroleum rock mechanics: Drilling operations and well design*. Gulf Professional Publishing, 2012. DOI: 10.1016/C2009-0-64677-8.

[14] Borivoje Pašić, Nediljka Gaurina-Medimurec, and Matanović Davorin, "Wellbore instability: Causes and consequences", *Rudarsko Geolosko Naftni Zbornik*, Vol. 19, No.1, 2007.

[15] Yufei Li, Yongqiang Fu, Geng Tang, Jianhua Guo, Jiyin Zhang, and Chaoyi She, "Effect of weak bedding planes on wellbore stability for shale gas wells", *IADC/SPE Asia Pacific Drilling Technology Conference and Exhibition, Tianjin, China, 9 - 11 July 2012*. DOI: 10.2118/155666-MS.

[16] Shiming He, Wei Wang, Jun Zhou, Zhen Huang, and Ming Tang, "A model for analysis of wellbore stability considering the effects of weak bedding planes", *Journal of Natural Gas Science and Engineering*, Vol. 27, pp. 1050 - 1062, 2015. DOI: 10.1016/j.jngse.2015.09.053.

[17] Brian Crawford, N.L. Dedontney, B. Alramahi, and S. Ottesen, "Shear strength anisotropy in fine grained rocks", *46th U.S. Rock Mechanics/Geomechanics Symposium, Chicago, Illinois, 24 - 27 June 2012*.

[18] Rajarajan Narayanasamy Naidu, D. Barr, A. MILNE, "Wellbore instability predictions within the Cretaceous mudstones, Clair field, West of Shetlands", *SPE Offshore Europe Oil & Gas Conference & Exhibition, Aberdeen, UK, 8 - 11 September 2009*.

[19] Chris Gallant, Jianguo Zhang, Christopher A. Wolfe, John Freeman, Talal Al-Bazali, and Mike Reese, "Wellbore stability consideration for drilling high-angle wells through finely", *SPE Annual Technical Conference and Exhibition, Anaheim, California, U.S.A., 11 - 14 November 2007*.